DEVELOPMENT AND TESTING OF NDE MOCKUP SPECIMENS WITH ASR

Eric R. Giannini[1]*, Patrice Rivard[2], Serge Apedovi Kodjo[2], Stepahnie G. Wood[1], Maria Guimaraes[3],

[1]The University of Alabama, Tuscaloosa, AL, UNITED STATES OF AMERICA

[2]Université de Sherbrooke, Sherbrooke, QC, CANADA

[3]Electric Power Research Institute, Charlotte, NC, UNITED STATES OF AMERICA

Abstract

A number of experimental NDT methods have provided promising results in evaluating small laboratory samples, often constructed of mortar and placed in severe environmental conditions. However attempts to apply these methods to larger-scale concrete specimens more dimensionally representative of concrete structures in the field have been more limited. A major challenge in validating NDT techniques for evaluating the severity of ASR-induced distress has been the lack of common specimens conditioned to a known level of deterioration. To address this problem, the Electric Power Research Institute (EPRI) and The University of Alabama partnered to fabricate and condition larger-scale plain concrete slabs to serve as common mockup specimens that were then made available to researchers to test the viability of their NDT methods. A research team from Université de Sherbrooke conducted non-linear acoustic testing (time-shift method) on the specimens at the EPRI NDE laboratories. The time-shift method was utilized to characterize distress in the specimens and was able to distinguish between specimens with varying degrees of expansion. This paper highlights the greater potential of nonlinear acoustics for assessing ASR damage.

Keywords: Nondestructive testing, alkali-silica reaction, ultrasonic pulse velocity, nonlinear acoustics, damage assessment

1 INTRODUCTION

Evaluation and monitoring of in-service structures affected by alkali-aggregate reactions remains a significant challenge to researchers and practicing engineers. Current methodologies rely heavily on surface crack mapping and long-term expansion measurements for in-situ monitoring, complemented by mechanical, chemical, and petrographic testing of core specimens in the laboratory. The utility of non-destructive testing (beyond visual inspection) has been limited at best. Non-destructive evaluation (NDE) methods that may be able to characterize ASR damage in small laboratory specimens are often unable to provide similar damage characterization for field structures [1].

However, in recent years, a number of studies have been conducted to develop new NDT methods. Most often, these have been performed on small specimens in the laboratory (e.g. 25 x 25 x 285 mm mortar bars) with severe exposure conditions (e.g. soaking in 1N NaOH at 80 °C) used to accelerate the development of damage from ASR. Many of these involve the analysis of non-linear acoustic responses to impact or resonant vibrations. Non-linear acoustic (NLA) measurements can be orders of magnitude more sensitive to the onset of damage from ASR than linear measurements (e.g. UPV). Unlike linear acoustics, which is primarily related to the elastic properties of materials, NLA is very sensitive to microscale changes, such as micro-cracking or changes at the interface between aggregate particles and cement paste. NLA involves applying high amplitude stress waves to a material; these introduce significant local deformations that cause nonlinear behavior by locally changing the elastic properties of the material over a short time scale, and the magnitude of this change is influenced by whether the material is damaged. Multiple variations of NLA exist and characterize the nonlinear behavior using different parameters [2-5].

There is a significant need to identify promising NDE methods capable of making the transition to use on large-scale or actual in-service structures. A major challenge to validating and vetting NDE techniques for evaluating the severity of ASR-induced distress has been the lack of

* Correspondence to: ergiannini@eng.ua.edu

common specimens conditioned to a known level of deterioration. To address this, researchers at The University of Alabama (UA) and the Electric Power Research Institute (EPRI) fabricated and conditioned four plain concrete slabs and smaller plain concrete prisms, and made these specimens available to NDE researchers for testing. These specimens serve as the first known set of shared mockup specimens for characterizing ASR damage using non-destructive methods. This paper presents information on the fabrication and conditioning of the specimen, along with the results of NLA tests performed by a team from Université de Sherbrooke.

2 MATERIALS AND METHODS

2.1 General

Four plain concrete slabs were constructed. Three were designed and conditioned to expand as from ASR; the fourth slab was constructed to serve as a non-expansive control specimen. Each slab had four small-scale accompanying prisms. The slab dimensions were 1220 x 915 x 200 mm and the prism dimensions were 102 x 76 x 406 mm. The specimens were then shipped to the Electric Power Research Institute (EPRI) NDE laboratory in Charlotte, North Carolina for testing by the Sherbrooke research team and made available to other NDE researchers.

The Sherbrooke team used nonlinear acoustics (NLA) to assess the level of damage in concrete. The NLA technique selected for the tests is the ultrasonic time shift [4,5]. This is a simple technique that consists of quantifying the influence of an external mechanical impact on the propagation of an ultrasonic wave. This technique, aside from the use of a dynamic load (impact), is similar to the acousto-elasticity technique [6], where the relative change of the ultrasonic wave velocity through a material charged under a static load is measured. The velocity variation is associated with the change in the elastic properties of the material.

2.2 Materials and mix designs

The materials used to create the reactive ASR specimens (ASR1, ASR2, and ASR3) included two reactive coarse aggregates from Wells, Maine (RCA1) and Bernalillo, New Mexico (RCA2), a highly-reactive fine aggregate from El Paso, Texas (RFA), and a Type I portland cement with a relatively high equivalent alkali content (Cement 1). Reactivity of all aggregates in this study was based on performance in the ASTM C1293 concrete prism test [7]. Sodium hydroxide (NaOH) was added to the reactive mixtures to obtain a 1.25% equivalent alkali content, by mass of cement. The non-expansive control mixture (ASR0) consisted of one non-reactive limestone coarse aggregate (NCA), a non-reactive limestone fine aggregate (NFA), and a low-alkali Type II portland cement (Cement 2). Both the NCA and NFA were acquired from a source in Calera, Alabama. The w/cm was 0.50 for all mixtures. Relevant material properties for mixture proportioning are listed in Table 1. Mixture proportions for the specimens are shown in Table 2.

Three batches of concrete (A, B, and C) were required for each slab and its matching prisms. The batches were mixed and placed in rapid succession to avoid the formation of cold joints. Slabs were vibrated in two layers using an internal vibrator, and the sides of the formwork were tapped with a rubber mallet to ensure consolidation, particularly in the corners. Slump, unit weight, and air content were determined for each batch in accordance with ASTM C143 [8], ASTM C29 [9], and ASTM C231 [10], respectively. Mixing temperatures were also recorded, and compressive strength tests were performed on 100 x 200 mm cylinders at 7 and 28 days following the guidelines of ASTM C39 [11] for quality control. Values for these properties, including average compressive strength, for each specimen are given in Table 3.

2.3 Methods for assessment and analysis

Specimen Conditioning

The slabs were moist-cured for seven days after casting. For the first four days, they were left in their formwork and covered with wet burlap. For the final three days, they were moved to an environmental chamber set at 23 °C and covered in wet burlap and plastic. The three accompanying prisms were demolded the day after casting and cured in a moist room at 23 °C and 100% relative humidity.

To induce ASR in the reactive slabs, condition in the environmental chamber were maintained at 27 °C and 65% relative humidity. This conditioning regime was less severe than standard accelerated laboratory tests; it was selected in order to prevent excessive expansions in the slabs because the aggregate combination had the potential to be extremely reactive. The temperature in the chamber was increased to 32 °C after taking readings at Day 93, but was returned back to 27 °C after taking readings on Day 107 because expansions in the slabs increased rapidly during that time. Slabs were draped with wet burlap and wrapped in plastic once per week after each expansion reading to maintain a supply of sufficient moisture. All matching prisms were kept in a moist curing room at 23 °C and 100% relative humidity. The non-reactive control slab remained was stored at a constant 23 °C and was draped in wet burlap weekly.

The three reactive specimens were conditioned in the environmental chamber until they reached target expansion levels of 0.05%, 0.10%, and 0.20%, respectively. Once specimens reached their target expansions, they were removed from the environmental chambers, packed, and shipped to the EPRI NDE laboratory in Charlotte, North Carolina (USA). At EPRI, specimens were stored indoors in a climate-controlled room maintained between 20 and 23 °C. The room was not humidified because the research team wanted to reduce the rate at which ASR was progressing in the specimens in order to maintain varying levels of damage present among the specimens.

Expansion Measurements

Specimen expansions were measured using the DEMEC system. A 500 mm-gauge length comparator was used to measure the expansion of the slabs and a 150 mm-gauge length comparator was used for the matching prisms.

The top surface of each slab had four DEMEC target discs arranged in a square (nominally 500 mm per side). Each side of the slabs had a pair of DEMEC targets spaced 500 mm apart and centered both vertically and horizontally. The targets on the sides of the slabs were conical divots machined into 9.5 mm-diameter hex bolts that were threaded into the formwork as shown in Figure 1. Vertical expansions of the slabs were not measured.

Three DEMEC discs were attached to each side of each matching prism for longitudinal expansion measurements. One disc was centered with the other two discs spaced at 150 mm from the center disc. Transverse expansions of the prisms were not measured.

Expansion measurements for the slabs and prisms were taken every seven days using a DEMEC gauge, as shown in Figure 2. Expansions on the top of the slabs were measured with the person taking measurements kneeling on top of the slab in the center of the DEMEC disc square. For reference purposes, each side of the slab was assigned a compass direction (i.e. north, south, east, and west). The ends of the matching prisms were also designated as north or south. The average expansions for each specimen were calculated as a simple average of the eight gauge lengths.

Nonlinear Acoustics (Time Shift Method)

The ultrasonic time shift technique uses the mathematical process of cross-correlation (eq. 1) between two signals recorded before the impact, s_0 (reference signal), and just after impact, s_i (disturbed signal). When changes occur in the medium due to the impact, a delay in the arrival time of the waves is observed in s_i.

$$C_{s_0 s_i}(\tau) = \int_{t'-t_w}^{t'+t_w} s_0(t) s_i(t-\tau) dt \qquad \text{(eq. 1)}$$

The time delay is processed from the correlation between both signals under a time window $2t_w$ centered at t'. The amplitude of the time delay depends on the amplitude of the deformation due to the impact. The time delay is equal to the value of τ which maximizes $C_{s_0 s_i}$.

The ultrasonic time-shift testing requires a signal generator with an integrated amplifier to generate pulses with duration of 30 μs and a rise time of 6 μs. These pulses excite a Panametrics piezoelectric longitudinal transducer V1012 with a central frequency of 250 kHz. Both receiver and transmitter transducer are placed on the same face of the specimen. The signal detected by the receiving transducer after propagation in the material and it is amplified before being sent onto an ADLINK PCI-9820 data acquisition board for digitization at a sampling rate of 60 MHz. The data acquisition system can record up to 125 signals (each 1 ms in length) per second. An impact produced with a short sledge impact hammer is applied on the surface of the sample while the ultrasonic pulses probe the medium. Honey was used as couplant between the transducers and the concrete surface. An accelerometer was glued underneath the specimen in order to record the response of the specimen in terms of vibrations. The accelerometer was glue to the specimen and honey was used for coupling the transducer to the specimen.

While the ultrasonic pulse probes the medium with the transducers attached on one side of the specimen, an impact is applied to the opposite surface of the specimen in order to perturb its elastic proprieties (Fig. 3). For each test, unperturbed probe signals were recorded before the impact, and perturbed probe signals were recorded after impact. The open and/or close cycles of micro-cracks due to the impact are evaluated by the time delay Δt between the signal before impact and the signal after impact. With a signal sampling rate of 60 MHz, the smallest value of Δt that was processed by the cross correlation function is about 10^{-8} s. Keeping the same configuration of transducers, it was assumed that the waves will travel the same path for each test; therefore a change of Δt is to be attributed solely to the damage in the concrete.

The signal is first filtered in order to remove the high-frequency noise and very-low-frequency before the cross-correlation process. To increase the sensitivity of the technique, the whole signal was analyzed. To do so, the signal was scanned with consecutive time windows of a specific width which is assumed large enough to take into account enough signal to improve correlation accuracy. For each step i of scan, Δt_i was processed.

The setup used for generating the probe wave through the prism specimens is the direct transmission (transducer emitter on one face and the receiver on the opposite face). Both transducers are attached at the end of the prism. With this configuration, the recorded probe signal contains the compressional wave arriving earlier in the signal (beginning of the signal) and the Coda part. The later contains a mix of P and S waves generated by multiple scattering of the ultrasonic waves on the inclusions, as well as the reflections from the borders. To process the data, the signal was scanned from 70 μs with consecutive time windows (width of 100 μs), which is assumed to be large enough to take into account sufficient signal length to improve the correlation accuracy. For each step i of the scan, Δt_i was processed through a cross correlation technique in the test procedure section.

3 RESULTS

3.1 Specimen Expansions

Figures 4 and 5 present the expansions with time for both the slabs and the specific prisms used for nonlinear acoustic testing. The figures are annotated with the expansion values of the specimens at the time they were shipped from Alabama to EPRI and the expansions at the time they were tested by the Sherbrooke team in December 2014. It can be seen that the reactive slabs were shipped just before reaching their target expansion values of 0.05%, 0.10%, and 0.20%. The prisms expanded less because of the cooler conditions in the curing room where they were stored. Figures 6 and 7 show examples of surface cracking observed on the specimens just prior to shipment to EPRI. During storage at EPRI, specimen size effects become evident. The reactive slabs continued to expand to between 0.13% and 0.20%, while the smaller matching prisms all shrank somewhat in dry storage.

3.2 Nonlinear Acoustics (Time-Shift Method)

Tests were performed at an age of 420 days for specimens ASR1, at 409 days for ASR3 and at 397 days for ASR0. Figure 8 shows the time shift calculated for the three slabs. One can observe that the control ASR0 have negligible time shift compared with slabs ASR1 and ASR3.

The time shift results obtained on prisms are shown in Figures 9 and 10. For both the compressional wave part and the Coda wave, the control specimen has very little time shift compared with the reactive specimens. Figure 9 shows the time shift of all prisms processed in the Coda part at 1240 μs of the signal. Figure 10 shows the average relative time shift using the full probe wave signal (the P-wave part and different parts of the Coda). The time shift calculated for prism ASR0 is negligible compared with the reactive specimens ASR1, ASR2, and ASR3.

4 DISCUSSION

The three reactive specimens were successfully conditioned at UA to different levels of damage from ASR, and continued to expand somewhat at EPRI prior to NDE measurements by the Sherbrooke research team. Logistical constraints prevented the Sherbrooke team from taking NDE measurements until approximately 10 months after the specimens arrived at EPRI.

Nonlinear acoustics appears to be very effective at low levels of damage. Previous studies have shown that nonlinear parameters change before concrete exhibit surface cracking [12, 13]. For the expansion levels of the concrete in this study, sensitivity of the time-shift method is much greater than would be expected from linear acoustic methods such as UPV or resonant frequency. Linear acoustic properties would only be expected to change by approximately 5 to 15%, based on the results reported by Giannini et al. [14]. At higher levels of damage, internal cracks are too wide; the nonlinear acoustic techniques become less sensitive. Other methods, based on linear acoustics (such as ultrasonic pulse velocity) can be more effective [15].

The force of the impact has a significant effect on the nonlinear behavior of the concrete. On small or medium-scale sample, a hammer appears to be sufficient to generate the opening/closing cycles of the cracks that generate the nonlinear behavior. However, on field structures, these results suggest that the amount of energy required might be greater to record time shift in the signal. Field studies are currently conducted to assess the suitability of the time shift method on service structures with vehicles that generate the impact on a bridge deck. Preliminary results suggest that such a procedure is suitable if the transducers are placed at points where deformations are greatest. Analysis of the vibration modes of the element is thus needed prior to installation of the transducers.

5 CONCLUSIONS

This study illustrates the potential of the nonlinear acoustic time-shift method to detect damage caused by ASR, both on large size slab and on small prisms. Several specific conclusions can be made based on the work presented in this paper:

- Negligible or no time-shift were measured for the non-reactive control specimens (ASR0).
- For the reactive slab specimens, time-shift increased with the impact force. The relative time-shift was greatest for reactive specimens with less expansion, and decreased for specimens with more expansion. This is consistent with prior work on the time-shift method.
- The time-shift method may therefore be considered of greatest utility when attempting to detect ASR in its early stages, before macro-cracking can be observed on the surface of the concrete, and perhaps even before micro-cracking develops.
- The utility of the time-shift method may also begin to decline once ASR advances to the point that many surface cracks can be easily seen with the naked eye. Greater expansions (e.g. >0.10%) produce wider, gel-filled cracks that reduce the interaction between the material on either side of the cracks. The nonlinear behavior of the concrete is highly-dependent upon these interactions, and this may explain the reduction in measured time shift.

6 REFERENCES

[1] Rivard, P, and Saint-Pierre, F (2008): "Alkali-silica reaction damage to concrete with non-destructive methods: From the lab to the field, Construction and Building Materials (23): 902-909.

[2] Ostravsky LA, and Johnson, PA (2001): Dynamic nonlinear elasticity in geomaterials. Rivista del Nuovo Cimento (24): 1-46.

[3] Van Den Abeele, KEA, Sutin, A, Carmeliet, J, and Johnson, PA (2001): Micro-damage diagnostics using nonlinear elastic wave spectroscopy (NEWS). NDT&E International (34) 239-248. doi:10.1016/S0963-8695(00)00064-5

[4] Bui, D, Kodjo, SA, Rivard, P, and Fournier, B (2013): Study of the time-shift technique in indirect and semi-direct transmission configurations for the evaluation of concrete structures subjected to distributed cracking. Journal of NDE (32): 25-36.

[5] Moradi-Marani, F, Kodjo, SA, Rivard, P, and Lamarche, CP (2014): Nonlinear acoustic technique of time shift for evaluation of ASR-damage in concrete structures. ACI Materials Journal (111)(5): 581-591.

[6] Lillamand, I, Chaix, JF, Ploix, MA, and Garnier, V (2010): Acoustoelastic effect in concrete material under uni-axial compressive loading. NDT&E International (43): 655-660.

[7] ASTM C1293-08b (2008): Standard Test Method for Determination of Length Change of Concrete Due to Alkali-Silica Reaction. ASTM International, West Conshohocken, PA, United States.

[8] ASTM C143-12 (2012): Standard Test Method for Slump of Hydraulic-Cement Concrete. ASTM International, West Conshohocken, PA, United States.

[9] ASTM C29-09 (2009): Standard Test Method for Bulk Density (Unit Weight) and Voids in Aggregate. ASTM International, West Conshohocken, PA, United States.

[10] ASTM C231-10 (2010): Standard Test Method for Air Content of Freshly Mixed Concrete by the Pressure Method. ASTM International, West Conshohocken, PA, United States.

[11] ASTM C39-12 (2012): Standard Test Method for Compressive Strength of Cylindrical Concrete Specimens." ASTM International, West Conshohocken, PA, United States.

[12] Chen, J, Jayapalan, AR, Kim, JY, Kurtis, KE, and Jacobs, LJ (2010): Rapid evaluation of alkali–silica reactivity of aggregates using a nonlinear resonance spectroscopy technique. Cement and Concrete Research (40): 914-923. doi:10.1016/j.cemconres.2010.01.003

[13] Boukari, Y, Rivard, P, Bulteel, D, and Ballivy, G (2012): Comparative study of nonlinear resonance and wave interaction techniques for concrete assessment. In: RILEM Bookseries (6):137-142.

[14] Giannini, ER, Folliard, KJ, Zhu, J, Bayrak, O, Kreitman, K, Webb, Z and Hanson, B (2013): Non-Destructive Evaluation of In-Service Concrete Structures Affected by Alkali-Silica Reaction (ASR) or Delayed Ettringite Formation (DEF)—Final Report, Part I. Report No. FHWA/TX-13/0-6491-1. Center for Transportation Research, Austin, TX.
[15] Sargolzahi, M, Kodjo, SA, Rivard, P, and Rhazi, J (2010) Effectiveness of nondestructive testing for the evaluation of alkali-silica reaction in concrete, Construction & Building Materials, 24(8): 1398-1403.

7 TABLES

TABLE 1: Material properties for cements and aggregates for mixture proportioning.

Material	Na_2O_{eq}, %	Absorption Capacity, %	Bulk Specific Gravity (Oven Dry)
Cement 1	1.10	-	3.15
Cement 2	0.53	-	3.15
RCA1	-	0.38	2.77
RCA2	-	0.60	2.64
NCA	-	0.70	2.74
RFA	-	1.10	2.57
NFA	-	1.00	2.70

TABLE 2: Mixture proportions for specimens.

Material	Quantity, kg/m^3	
	ASR Reactive	ASR Control
Cement 1	420	-
Cement 2	-	420
Water	210	210
RCA1 (oven dry)	429	-
RCA2 (oven dry)	429	-
NCA (oven dry)	-	1095
RFA (oven dry)	818	-
NFA (oven dry)	-	639
NaOH	1.63	-

TABLE 3: Average air content and compressive strength for each specimen.

Specimen	Air Content, %	Compressive Strength, MPa	
		7 Days	28 Days
ASR1	1.7	30.5	40.5
ASR2	1.9	29.8	39.1
ASR3	1.8	32.6	40.0
ASR0	1.1	37.7	42.8

8 FIGURES

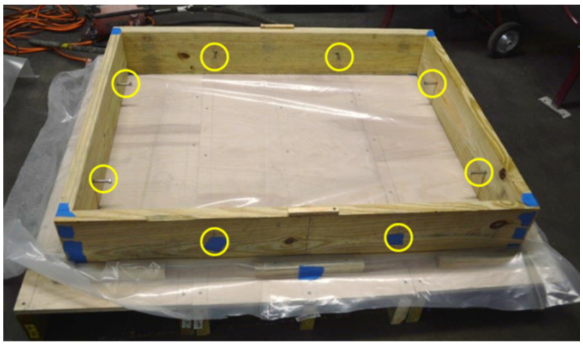

FIGURE 1: Formwork for a slab. Yellow circles indicate locations of hex bolts.

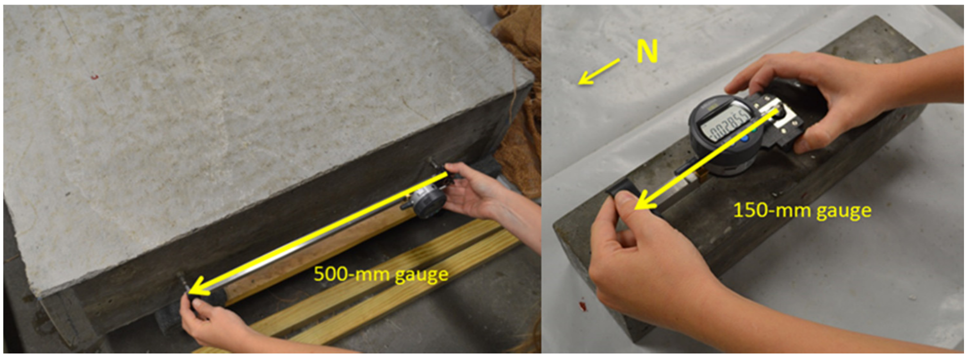

FIGURE 2: Measuring orientation of slabs (left) and ASR matching prisms (right).

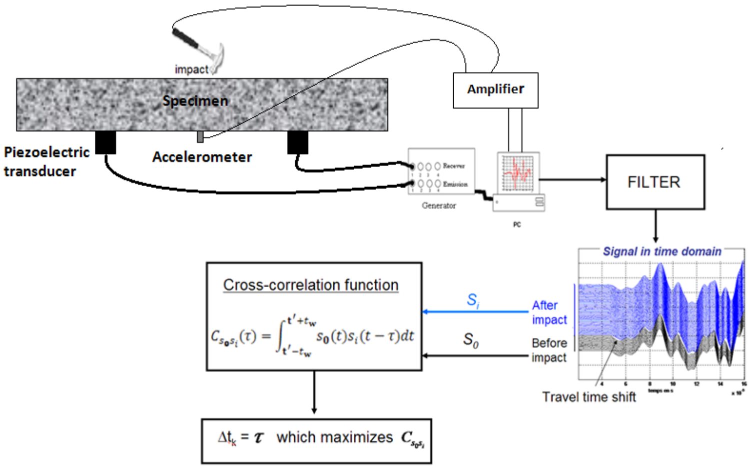

FIGURE 3: Nonlinear time shift procedure sketch for measurement on the slab.

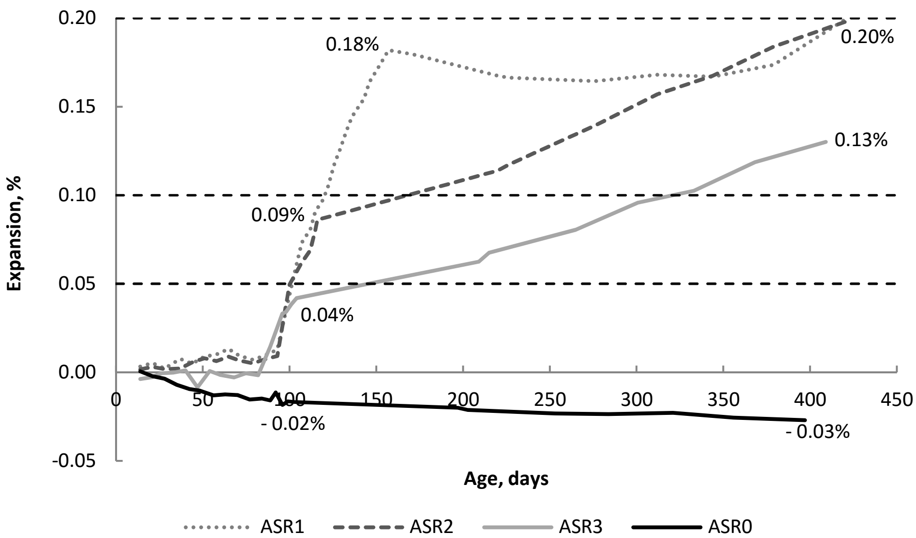

FIGURE 4: Expansions with time for the slabs. Horizontal dashed lines indicate target expansions for the reactive slabs. Expansion values are given for when the specimens were shipped to EPRI and when they were tested by the Sherbrooke team.

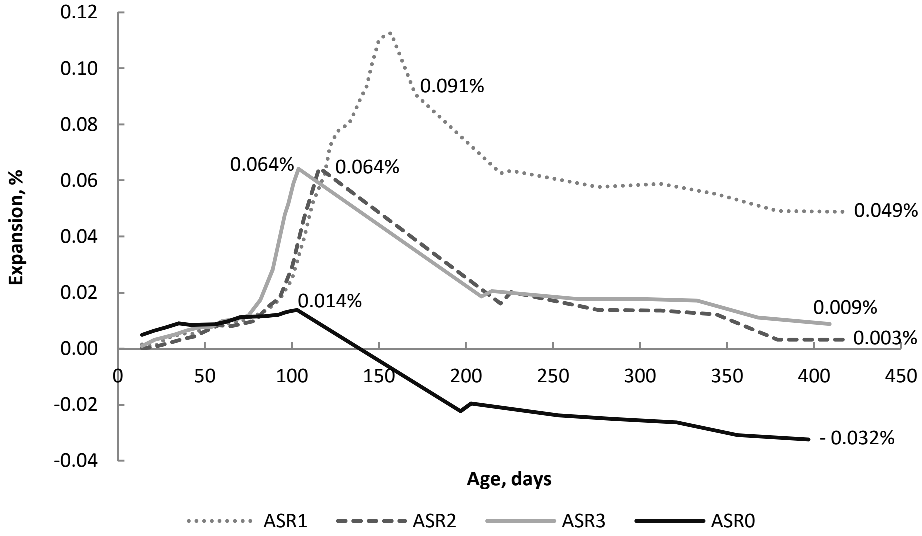

FIGURE 5: Expansions with time for the selected matching prisms used for NLA testing. Expansion values are given for when the specimens were shipped to EPRI and when they were tested by the Sherbrooke team.

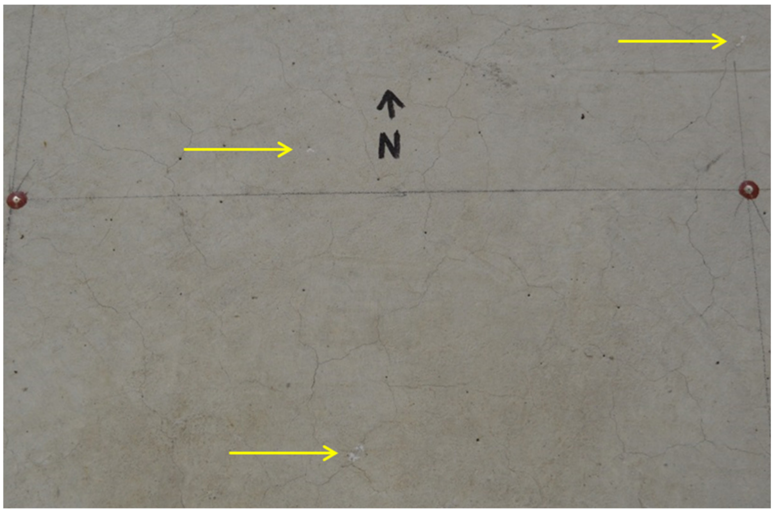

FIGURE 6: Map cracking and efflorescence on the top of a slab. Yellow arrows indicate areas of efflorescence.

FIGURE 7: Cracking and efflorescence on a matching prism.

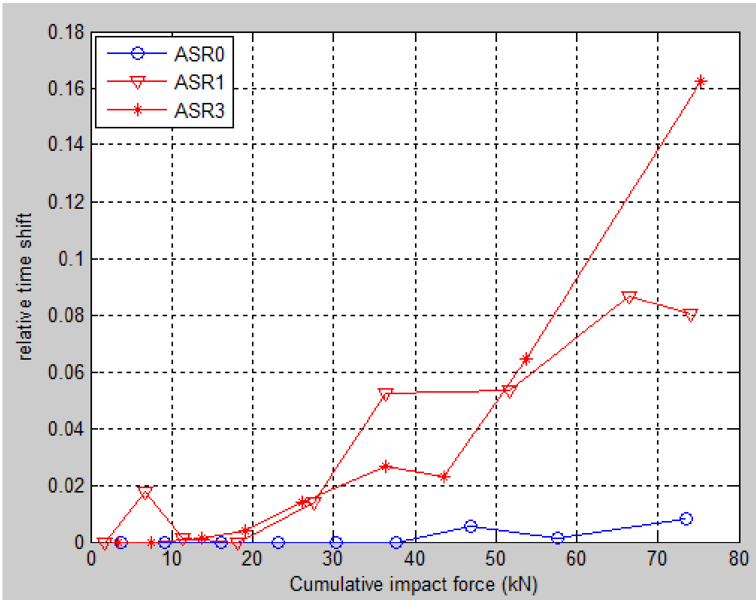

FIGURE 8: Time shift calculated from slab specimens.

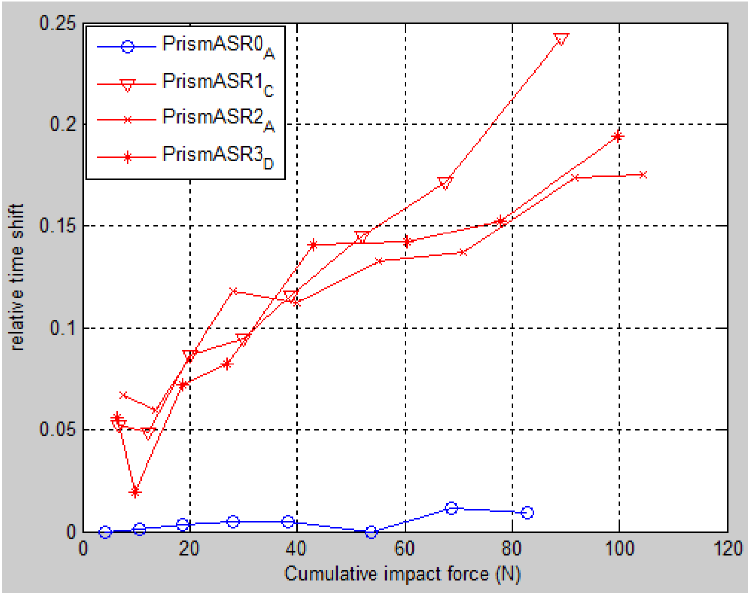

FIGURE 9: Time shift calculated for all ASR prism specimens (Coda).

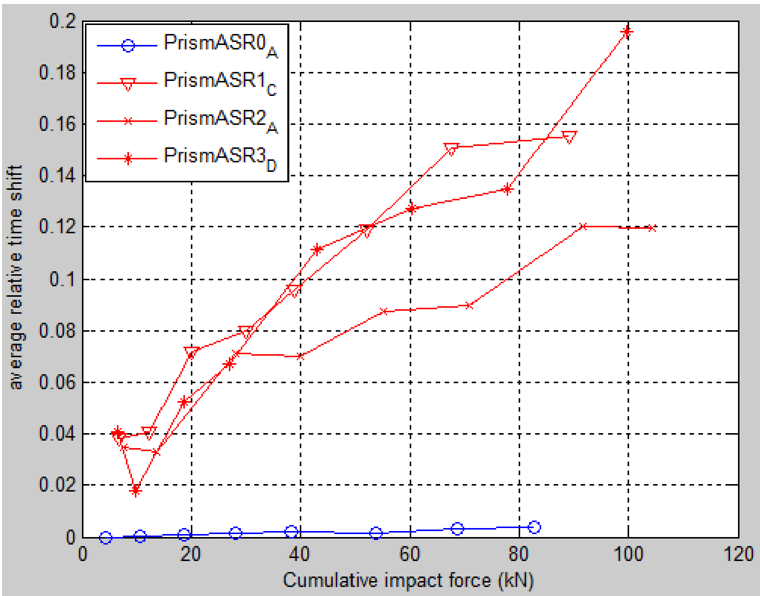

FIGURE 10: Average relative time shift for ASR prisms calculated from the whole signal.